UDC 629.7.036.74 DOI: 10.18698/0236-3941-2021-1-53-67

METHODS FOR ASSESSING PARAMETERS OF THE STATIONARY PLASMA ENGINE PLUME MULTIFRACTIONAL MODEL BASED ON THE RESULTS OF PROBE MEASUREMENTS

A.B. Nadiradze[1] nadiradze@mai.ru
Yu.L. Frolova[2] ylfrolova@yandex.ru

[1] Moscow Aviation Institute (National Research University), Moscow, Russian Federation
[2] VNIIMS, Moscow, Russian Federation

Abstract

Methods are presented for determining parameters of the stationary plasma thruster (SPT) multifractional conical plume model using the electrostatic probing analyzer braking characteristics with retarding potential. Processing is carried out in three stages. At the first stage, braking characteristics are smoothed using the cubic splines. Node initial position is determined by the piecewise linear approximation nodes. Then, optimization problem is being solved, and node position is found, spline minimum deviation from the experimental curve is achieved in the absence of points with positive derivative. At the second stage, plume ions are divided into monoenergetic fractions. Division is carried out by the inverse function method with respect to the plume ions integral distribution function. At the third stage, fraction angular characteristics are smoothed together. To ensure constancy of the fraction current density total values, which could be violated with separate smoothing, special functions are introduced to separate the fractions. These functions divide the plume ions into two parts according to the retarding potential value corresponding to the fraction boundaries. Separation functions are being smoothed, and a set of smoothed angular characteristics of each fraction is obtained using these functions. In this case, the total fraction current density is not changing. Obtained distributions are used as parameters of a plume multifractional conical model suitable for engineering analyzes of the stationary plasma thruster on a spacecraft. Smoothing eliminates irregularity in angular and energy distributions caused by the measurement error and makes it possible to exclude probable artifacts appearing from analyzing results of the stationary plasma thruster plume impact on the spacecraft elements and systems

Keywords

Stationary plasma thruster, plume multifractional model, electrostatic probe — energy analyzer, braking characteristic, angular characteristic, smoothing

Received 23.06.2020
Accepted 14.09.2020

Introduction. Stationary plasma thrusters (SPT) are widely used on board the modern spacecraft (SC) [1–3]. However, high velocities of the particles outflow and their ionized state bring about a situation, where an SPT plume could interact intensively with the SC outer surface materials and its systems [4–6] leading to a decrease in the SC useful life and operational characteristics. In this regard, one of the most important tasks in using an SPT in space is to ensure compatibility of the SPT with the SC elements and to minimize negative consequences of the SPT plasma plume impact on the spacecraft.

It is obvious that solution to this problem is impossible without detailed study and construction of the SPT plume mathematical model, which provides a sufficiently high accuracy of calculations.

Currently, there are many SPT plume mathematical models from the simplest semi-empirical to those complex kinetic [7–9]. However, complexity of the processes occurring in the discharge region and in the region of SPT cathode plasma still does not make it possible to obtain a model with sufficiently satisfactory predictive qualities and coinciding with the experimental data. In this regard, semi-empirical models being constructed on the results of experimental measurements of the specific thruster model plume parameters are generally used in engineering analysis of the SPT plasma plume impact on a SC.

The most reliable data could be obtained only under full-scale conditions of a spacecraft operation. However, direct measurements in space are meeting significant difficulties due to restrictions in number and position of sensors measuring the plume parameters, as well as to significant material costs. The number of flight experiments implemented at the present time is counted in units. The first flight tests of an SPT were carried out back in the 1970s during flights of the Meteor and Meteor-Priroda meteorological satellites [10]. Most detailed measurement of the plasma plume parameters in space were carried out on board two Express-A geostationary communication satellites [11]. However, all the data obtained in flight experiments do not allow compiling an exhaustive description of the SPT plasma plume. And it is unlikely that this situation would be radically changed in the coming years despite the fact that equipment for plume research is being improved, and new flight experiments are planned [12].

Plume parameter measurement in bench testing is much more comprehensive and informative [13–15]. However, it is practically impossible to fully simulate in ground testing those environmental conditions typical for the thruster operation in space. Therefore, measurement results are distorted. To implement measurements in conditions that are closest to the real ones, super-powerful pumping equipment with a capacity of more than 200 000 l/s [16] is required, which is difficult to achieve even at the current level of technology. Moreover, there appeared a tendency in the recent years to create powerful SPTs [17] to be introduced in the interplanetary flights and in solving the tasks of final ascent. When testing such engines in vacuum chambers, significant errors in the measurements of thrust and plume parameters arise [18–20], which could not be ignored.

Solution to the problem is possible only by creating an end-to-end kinetic model of the SPT working processes and the plume outflowing from it. This model should allow interpreting results of the bench measurements and correctly extrapolating them to conditions of a spacecraft flight operation [20, 21]. Until such a model is created and verified, engineering calculations of the SPT plasma plume effect on the spacecraft would be carried out using the simple semi-empirical models based on experimental data obtained under bench conditions.

One of such models is the multifractional conical plume model [22]. This model is based on the point source and makes it possible to describe the complex angular and energy distribution of ions in the SPT plume. At the same time, it should be noted that the SPT plume is not strictly conical. Works [23, 24] convincingly prove that plasma at distances of more than one or two meters from the thruster expands faster than $1/r^2$. Moreover, this circumstance also finds experimental confirmation [24]. This factor should be taken into account when calculating plume parameters at large distances from the thruster. But the use of a conical model is quite justified within a radius of three to five meters, where the plume has the greatest impact on a spacecraft, and deviations from the conical shape are insignificant [25].

The purpose of this article is to review the methods that were applied and improved by the authors during many years of practical work on the named model. As of today, these methods acquired certain completeness, and we would like to present them to the scientific community.

Basic provisions of the SPT plume multifractional model. When constructing the SPT plume multifractional conical model of the SPT plume, it is assumed that plume particles move without collisions along the rays emanating from the center of the thruster outlet section. In this case, any exchange of energy, mass and charge between the plume particles is missing. Plume particles are divided into the M monoenergetic fractions. Each fraction is characterized by the q_f charge and the energy range $(E_f,\ E_{f+1})$, where $f = 0, \ldots, M$ is the fraction index. Angular particle distribution in each fraction is set by the point source model:

$$n_f(r,\varphi) = n_{0,f}(\varphi)\left(\frac{r_0}{r}\right)^2,$$

where $n_f(r,\varphi)$ is concentration of particles of the *f*-th fraction at the *B* (r, φ); r is the distance from the thruster to point *B* along the r ray; φ is the angle of ray deflection from the plume axis; $n_{0,f}(\varphi)$ is the initial concentration of particles of the *f*-th fraction at the $r = r_0$ distance from the thruster.

This model could be applied at a sufficiently large distance from the thruster (at $r \geq (5-10)R_{mid}$, where R_{mid} is the radius of the SPT discharge channel central line), where the source geometric shape and collisions between the plume particles are no longer affecting the flow parameters.

To determine parameters of this model, measurement results are usually used of the current density and the ion energy distribution function under bench conditions obtained using the electrostatic probes — energy analyzers (hereinafter referred to as the probes) [26]. When carrying out measurements, probes are positioned at the same r_0 distance from the source at the φ_k different angles to the plume axis. By varying the retarding potential value on the probe control grid, the so-called $I_{>E,k}(E)$ inhibitory characteristic is obtained, which characterizes the plume ion distribution function over the $f(E, \varphi_k)$ energies:

$$I_{>E,k}(E) = j(\varphi_k)\,S_{eff}\int_E^{\infty} f(E, \varphi_k)\,dE,$$

where $I_{>E,k}$ is the probe collector current; $j(\varphi_k)$ is the ion current density at the probe position *k*-th point; *E* is the energy of the ion, $E = qU$, *U* is the retarding potential on the control grid; S_{eff} is the probe effective area.

Since the electrostatic energy analyzer does not allow distinguishing particles of different charge and masses, it is more convenient instead of the function of ion distribution over the $f(E, \varphi_k)$ energies to use distribution over the $f(U, \varphi_k)$ retarding potential value:

$$I_{>U,k}(U) = j(\varphi_k)\,S_{eff}\int_U^{\infty} f(U, \varphi_k)\,dU.$$

In this case, uncertainty in the q value arising in the presence of particles of different charges in the plume disappears. For the same reasons, separation of particles into fractions is carried out according to the *U* retarding potential value. The resulting “mixture” of particles with different q in a single fraction is taken into account by introducing the concepts of the fraction charge composition and subsequent division of fractions into the charge components.

As is known [27], charge composition could vary depending on the particle emission angle. But taking into account significant uncertainty in this parameter and its relatively insignificant effect on the plume parameters, it is assumed that charge composition is constant at all points of the plume. In this case, the flux density and the current density of the *i*-th charge component particles of the *f*-th fraction would be determined by the following relations:

$$nv_{f,i} = \mu_i nv_f;$$

$$j_{f,i} = j_f \frac{\mu_i q_i}{\overline{q}},$$

where $\overline{q} = \sum_i \mu_i q_i$ is the plume ion average charge; μ_i is the fraction of the mass flow of particles of the *i*-th charge component having the $q_i = ie$ charge, and $\sum_{i=1}^{i=L} \mu_i = 1,$ where *L* is the number of charge components; *e* is the electron charge.

Average speed and concentration of particles of the *i*-th charge component of the *f*-th fraction, respectively, are equal:

$$v_{f,i} = \sqrt{(U_f + U_{f+1})\frac{q_i}{m_1}};$$

$$n_{f,i} = \frac{j_{f,i}}{v_{f,i}\, q_i},$$

where m_1 is the ion mass.

Total concentration of particles of all the fraction charge components is:

$$n_f = \frac{j_f}{\overline{q}} \sum_i \frac{\mu_i}{v_{f,i}}.$$

Total ion current density at the probe installation point (at the $r = r_0$ distance from the thruster) is determined from the braking characteristic as:

$$j_i(\varphi_k) = \frac{I_{>U,k}(0)}{S_{eff}},$$

and total current density of particles of the *f*-th fraction is:

$$j_f(\varphi_k) = j_i(\varphi_k)\frac{I_{>U,k}(U_{f+1}) - I_{>U,k}(U_f)}{I_{>U,k}(0)};$$

$$j_i(\varphi_k) = \sum_f j_f(\varphi_k),$$

where U_f, U_{f+1} are the boundary values of retarding potential for particles of the f-th fraction.

Thus, it becomes possible using the $I_{>U,k}(U)$ braking characteristics set and the S_{eff} value to calculate the fraction parameters. And knowing the $\{\mu_i\}^L$ plume charge composition, also to calculate the charge components parameters.

Plume ions division into fractions. To divide ions of the plume into fractions, let us use the inverse function method. It is required that the ion current of each fraction is equal to I_i / M, where I_i is the total ion current of the plume. Then, for the retarding potential boundary values of the U_f fractions, the following is obtained:

$$U_f = F^{-1}\left(\frac{M-f}{M}\right), \; f = 0, \ldots, M,$$

where $F(U)$ is the integral distribution function for all ions in the plume, which is determined by the following relation:

$$F(U) = \frac{\int\limits_{\varphi} I_{>U}(U,\varphi)\sin(\varphi)\,d\varphi}{\int\limits_{\varphi} I_{>U}(0,\varphi)\sin(\varphi)\,d\varphi}.$$

An example of the BHT-1500 thruster engine plume ions division into fractions with the thruster operating in the 700 V [21] mode is shown in Fig. 1.

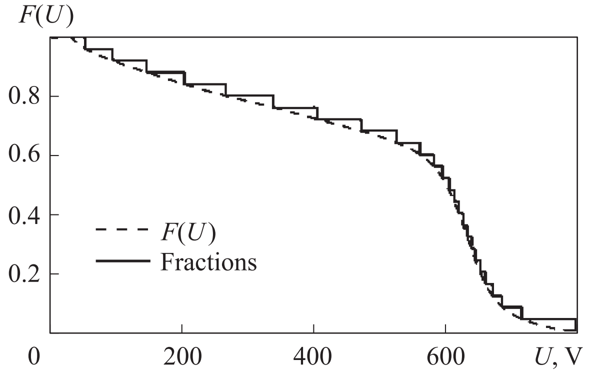

Fig. 1. Integral distribution function of the $F(U)$ plume ions and its division into fractions (25 fractions)

It was experimentally established that the most rational is the plume ions division into 15–30 fractions.

Smoothing the braking characteristics. The $I_{>U,k}(U)$ initial braking characteristics, especially at the large φ angles, are usually very noisy (Fig. 2), and in this connection it becomes necessary to smooth them.

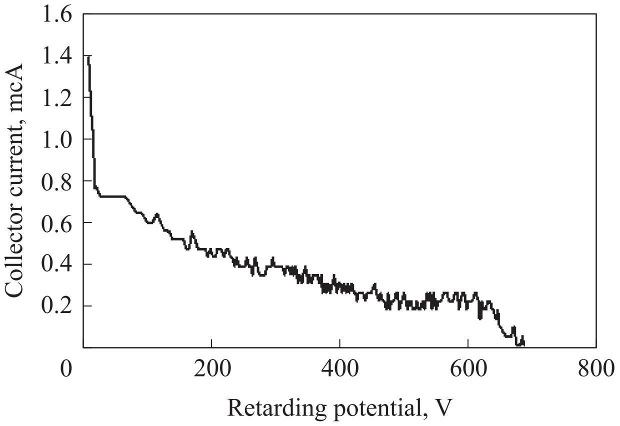

Fig. 2. Typical braking characteristic of an electrostatic probe-energy analyzer in the plume peripheral zone

Using standard smoothing techniques such as cubic splines, for example, often leads to inconsistent situations, where the $\frac{d}{dU} I_{>U,k}(U)$ derivative is higher than zero. Selection of the interpolation nodes number and position also plays an important role in the smoothing quality. An algorithm is proposed to solve these problems that uses piecewise-linear approximation to select interpolation nodes and cubic smoothing splines to construct the desired approximating function.

Let us proceed from the fact that the $I_{>U,k}(U)$ values were measured with a ε_I certain error. Let us denote by $y = I_{>U,k}(U)$ and $x = U$. Results of the $y(x)$ measurement have the form of the $D\{x_i, y_i\}^N$ array, where N is the array elements number. Let us find the $g_m(x)$ continuous piecewise linear function approximating the $y(x)$ and meeting the following criterion:

$$\Delta_{\max} = \max\left|g_m(x) - y(x)\right| \le \varepsilon_I,\ x = x_0, \ldots, x_{N-1}. \tag{1}$$

Let us limit the number of the $g_m(x)$ nodes by the required minimum and require that $g_m(x_i) \ge g_m(x_{i+1})$.

In this case, algorithm for constructing the $g_m(x)$ could be realized as a sequential recursive division of the $[a, b]$ segment by the $c = x_i$ intermediate point from the D array, such as:

$$c = \underset{x_i \in (a,b)}{\arg\max} \left(\left| g_m(x_i) - y(x_i) \right| \right).$$

The $\left[x_0, x_{N-1}\right]$ segment is taken at the first iteration, and the x_i division point is found. Then the left $\left[x_0, x_i\right]$ and the right $\left[x_i, x_{N-1}\right]$ segments are divided. Fulfillment of the $g_m(x_i) \geq g_m(x_{i+1})$ condition is checked on every segment, and possible contradictory situations are excluded. Segment division continues recursively, if condition (1) is not satisfied there. An example of division is presented in Fig. 3.

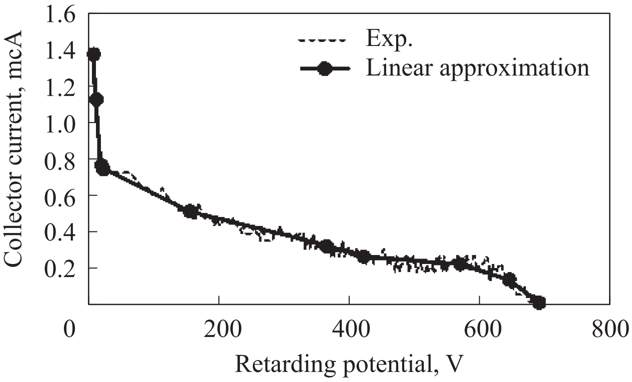

Fig. 3. Braking characteristic approximation by the piecewise linear function (10 nodes)

The $g_m(x)$ resulting function is not contradicting with $\frac{d}{dx} g_m(x) \leq 0$ and meets requirement for the $\Delta_{\max} \leq \varepsilon_I$ approximation accuracy. However, discontinuities in the derivative do not allow using it to determine the model parameters. In this regard, the $y(x)$ is approximated at the next stage by the $S_p(x)$ cubic smoothing spline [27] constructed on the $g_m(x)$ function nodal points. It is assumed at the segment boundaries that $S_p(0) = 0$ and $S_p(U_{\max}) = 0$, where $U_{\max}$ is the right boundary of the braking characteristic.

To exclude the $g_m(x)$ segments with negative derivative (contradictory situations), the interpolation nodes position is corrected by solving the optimization problem:

$$\left\{x_{b,j}, y_{b,j}\right\}^L = \arg\min(\Omega); \tag{2}$$

$$\Omega = \sum_i \left(S_m(x_i) - y_i(x_i)\right),$$

where $\left\{x_{b,j}, y_{b,j}\right\}^L$ is the interpolation node array.

Solution (2) is being sought with the coordinate descent method by sequentially varying position of the interpolation nodes within the boundaries. Intermediate node position is varying within the boundaries determined by position of the nodes adjacent to them. Approximation results are presented in Fig. 4.

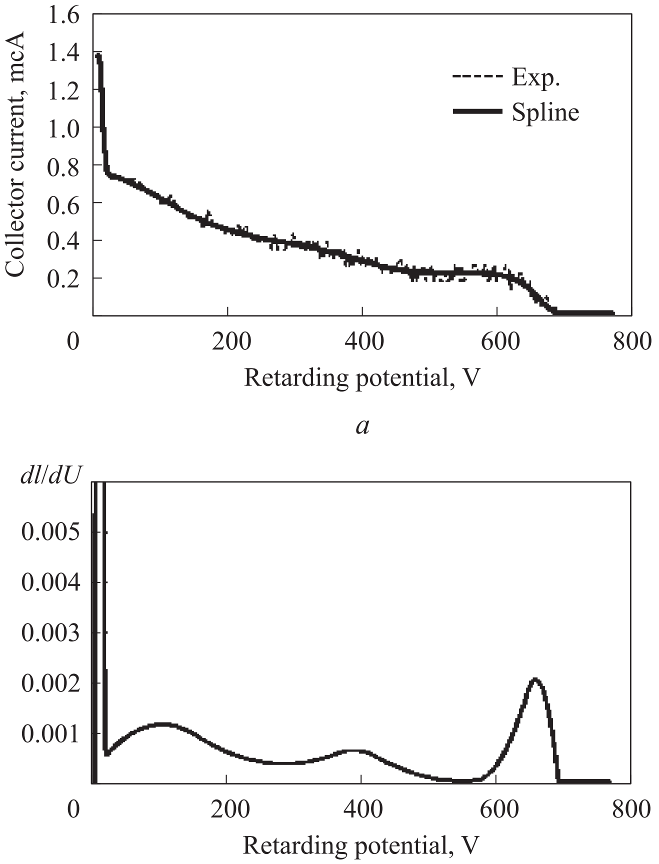

a

b

Fig. 4. Braking characteristic approximation by a smoothing cubic spline (*a*) and its corresponding distribution function (*b*)

Approximation of angular distributions. After smoothing the braking characteristics, let us pass to smoothing the $j_f(\varphi)$ fraction angular distributions. Requirement for such smoothing is due to the fact that using the braking characteristics “as they are” leads to obtaining the resulting set of fraction angular distributions being significantly irregular (Fig. 5). Before starting to smooth angular distribution of fractions, let us approximate the $j_i(\varphi)$ plume ions angular distribution by the smoothing spline [27].

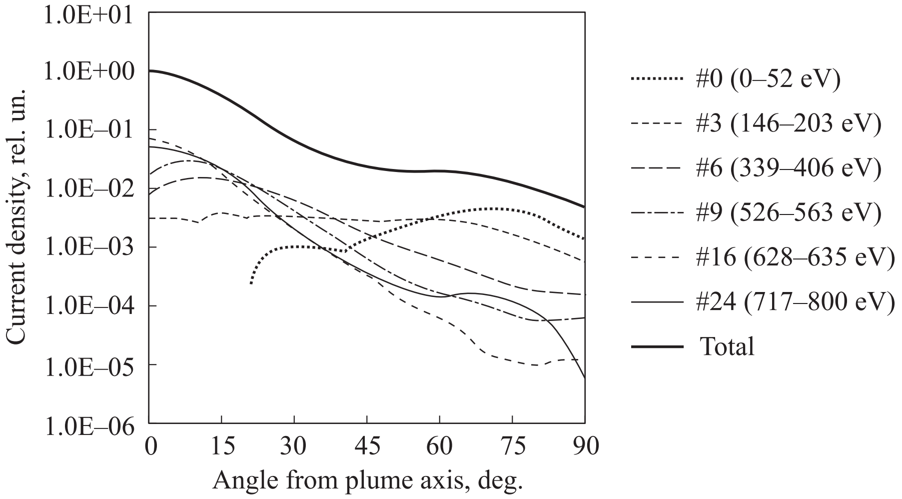

Fig. 5. Fraction angular distribution without using the smoothing procedure

To smooth the angular distributions, let us introduce the fractions dividing angular function by the retarding potential value:

$$\gamma_f(\varphi)=\frac{I_{>U}(U_f,\varphi)}{I_{>U}(0,\varphi)},\quad f=0,\ldots,M.$$

Then, angular distribution of the ion current density in each fraction could be represented as:

$$j_f(\varphi)=\tilde{j}_i(\varphi)\,\eta_f(\varphi),$$

where $\eta_f(\varphi)=\gamma_f(\varphi)-\gamma_{f+1}(\varphi)$ are the weight functions characterizing the f-fraction ion content in the flow; $\tilde{j}_i(\varphi)$ is the smoothed angular distribution of the plume ions.

Let us note that $\gamma_0(\varphi)=1$, $\gamma_M(\varphi)=0$ and $0\le\eta_f(\varphi)\le 1$; and for the $\eta_f(\varphi)$ entire collection the following condition is being fulfilled:

$$\sum\eta_f(\varphi)=1. \tag{3}$$

If the smoothing procedure is applied to $\eta_f(\varphi)$, condition (3) could be violated. Therefore, the smoothing procedure would be applied to $\gamma_f(\varphi)$. To eliminate contradictory situations (where $\eta_f(\varphi)<0$ or $\eta_f(\varphi)>1$), coincidence is required in the values of spline and $\gamma_f(\varphi)$ function at the edges of the φ angle range of values.

As an example, Fig. 6 presents the $\gamma_f(\varphi)$ initial values obtained from the data in work [21], and the result of approximation thereof by the smoothing splines [27]. Fig. 7 shows the fraction angular distributions obtained from the smoothed $\gamma_f(\varphi)$.

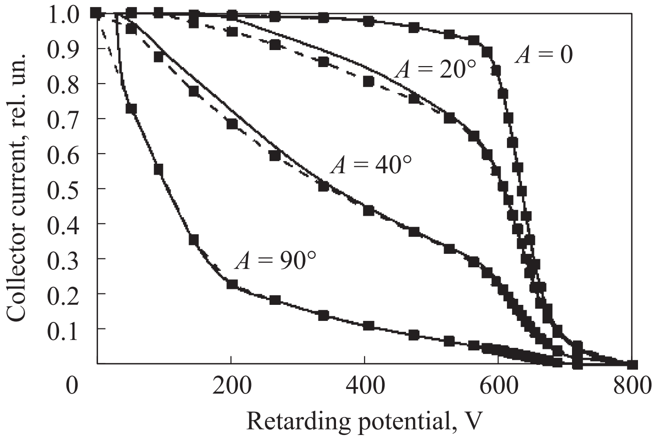

Fig. 6. Initial (markers and dashed curves) and smoothed (solid curves) values of the fraction division functions

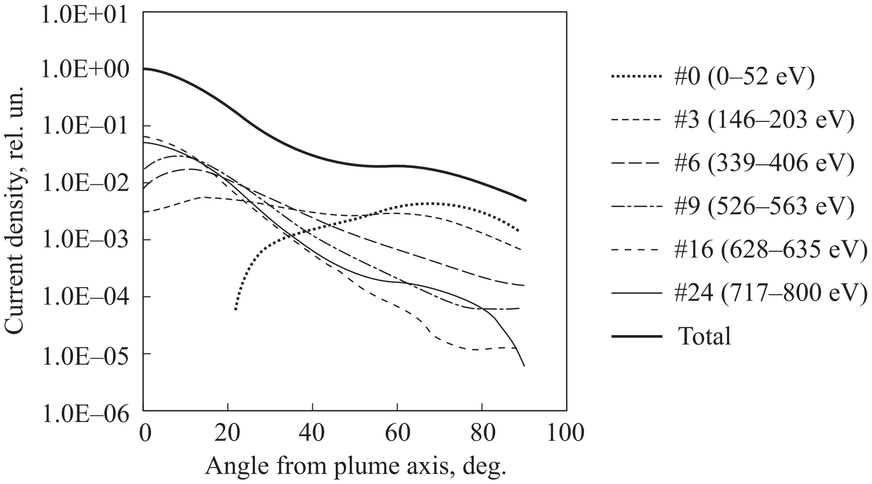

Fig. 7. Angular fraction distributions after applying the smoothing procedure

Since the fraction current density alteration ratio changes during smoothing, the ions energy spectra of ions reconstructed from the fraction parameters would differ from the initial spectra (Fig. 8).

As braking characteristics were measured with an error, it is still rather difficult to indicate, which of these spectra are closer to the true ones.

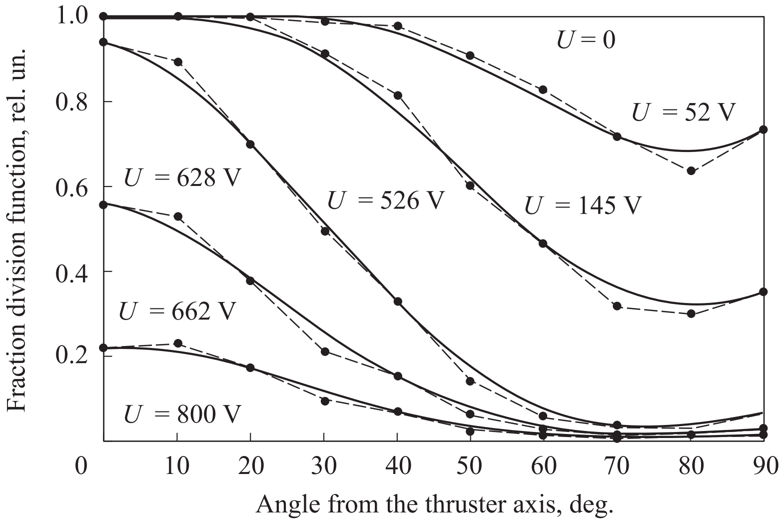

Fig. 8. Braking characteristics before (markers and dashed curves) and after (solid curves) applying the smoothing procedure

Since when constructing a plume model based on the braking characteristics, significant discrepancies between the plume and the thruster integral parameters could appear [28], the model is being calibrated after the smoothing procedure [29]. Thruster integral parameters and efficiency factors are determined by the method [30].

Conclusions. Methods are presented for determining the multifractional conical plume model parameters using the electrostatic probes — energy analyzers braking characteristics measured at different angles from the plume axis. Experimental data are processed in three stages. At the first stage, the braking characteristics are being smoothed. At the second, the plume ions are divided into monoenergetic fractions. At the third stage, combined smoothing of the fraction angular distributions is performed. Obtained distributions are used as parameters of the multifractional conical plume model suitable for engineering analyzes of the SPT plasma plume impact on a spacecraft. Smoothing eliminates unevenness in angular and energy distributions caused by the measurement error and makes it possible to exclude probable artifacts from the results of analysis.

Translated by K. Zykova

REFERENCES

[1] Gorshkov O.A., Murav’yev V.A., Shagayda A.A. Kholovskie i ionnye plazmennye dvigateli dlya kosmicheskikh apparatov [Hall and ion plasma engines for spacecraft]. Moscow, Mashinostroenie Publ., 2008.

[2] Kim V. Stationary plasma thrusters in Russia: problems and perspectives. *Trudy MAI*, 2012, no. 60 (in Russ.). Available at: http://trudymai.ru/published.php?ID=35374

[3] Arkhipov A.S., Kim V.P., Sidorenko E.K. Statsionarnye plazmennye dvigateli Morozova [Morozov stationary plasma engines]. Moscow, MAI Publ., 2012.

[4] Kim V.P., Nadiradze A.B., Popov G.A., et al. Problemy primeneniya elektroraketnykh dvigateley na kosmicheskikh apparatakh. V: Model' kosmosa. T. 2. Vozdeystvie kosmicheskoy sredy na materialy i oborudovanie kosmicheskikh apparatov [Problems of electric propulsion thruster application in spacecraft. In: Model of the space. Vol. 2. Effect of space environment on spacecraft materials and equipment]. Moscow, Universitet Publ., 2007, pp. 615–659 (in Russ.).

[5] Korsun A.G., Tverdokhlebova E.M., Novikov G.I., et al. Voprosy zashchity kosmicheskikh apparatov ot elektrofizicheskogo vozdeystviya. Sistemnaya ballistika i effektivnost' kosmicheskikh sistem distantsionnogo zondirovaniya Zemli [Issues of protecting spacecraft and equipment from electrophysical effects. System ballistics and space systems efficiency for Earth remote sensing]. Moscow, ZAO NII Entsitekh Publ., 2012.

[6] Khodnenko V.P. Impact of stationary plasma thrusters on “Electro-M” and “Electro-M1” satellites operability. *Voprosy elektromekhaniki. Trudy VNIIEM* [Electromechanical Matters. VNIIEM Studies], 2018, vol. 164, no. 3, pp. 44–46 (in Russ.).

[7] Goebel D.M., Katz I. Fundamentals of electric propulsion: ion and hall thrusters. Chichester, John Wiley & Sons, 2008.

[8] Arkhipov A.S., Bishaev A.M. Three-dimensional numerical simulation of the plasma plume from a stationary plasma thruster. *Comput. Math. and Math. Phys.*, 2007, vol. 47, no. 3, pp. 472–486. DOI: https://doi.org/10.1134/S0965542507030116

[9] Merino M., Cichocki F., Ahedo E. A collisionless plasma thruster plume expansion model. *Plasma Sources Sc. Technol.*, 2015, vol. 24, no. 3, art. 035006.
DOI: https://doi.org/10.1088/0963-0252/24/3/035006

[10] Artsimovich L.A., Andronov I.M., Morozov A.I., et al. Development of a stationary plasma thruster (SPT) and its testing on “Meteor” satellite. *Kosmicheskie issledovaniya*, 1974, vol. 12, no. 3, pp. 451–468 (in Russ.).

[11] Manzella D. Hall thruster plume measurements onboard the Russian express satellite. *27th IEPC*, 2001, art. IEPC-01-044.

[12] Laube J., Trottenberg T., Bansemer F., et al. Development of a flight electric propulsion diagnostic package (EPDP) for EP satellite platforms. *The 36th Int. Electric Propulsion Conf.*, 2019, art. IEPC-2019-345.

[13] Absalamov S.K., Andreev V.B., Colbert T., et al. Measurement of plasma parameters in the stationary plasma thruster (SPT-100) plume and its effect on spacecraft components. *AIAA/SAE/ASME/ASEE 28th Joint Propulsion Conf.*, 1992, art. AIAA-92-3156. Available at: https://doi.org/10.2514/6.1992-3156

[14] Pagano D., Scaranzin S., Meniconi G., et al. Performance and plume characterization of the SPT100-B thruster. *Joint Conf. 30th ISTS, 34th IEPC and 6th NSAT*, 2015, art. IEPC-2015-010.

[15] Kim V., Kozlov V., Popov G., et al. Plasma parameter distribution determination in SPT-70 plume. *Proc. 28th Int. Electric Propulsion Conf.*, 2003, art. IEPC-2003-107.

[16] Boyd I.D., Cai C., Walker M.L.R., et al. Computation of neutral gas flow from a hall thruster into a vacuum chamber. *Rarefied Gas Dynamics. 23rd Int. Symp.*, 2002, pp. 541–548.

[17] Boykachev V.N., Gusev Yu.G., Zhasan V.S., et al. On the possibility to develop a 10 to 30 kW electric propulsion system based on dual-mode thruster SPD-140D. *Kosmicheskaya tekhnika i tekhnologii* [Space Technique and Technologies], 2014, no. 1, pp. 48–59 (in Russ.).

[18] Snyder J.S., Lenguito G., Frieman J.D., et al. The effects of background pressure on SPT-140 thruster performance at multiple power levels. *53rd AAA/ASME/SAE/ASEE Joint Propulsion Conf.*, 2008. DOI: https://doi.org/10.2514/6.2018-4421

[19] Ortega A.L., Mikellides I.G., Chaplin V.H., et al. Facility pressure effects on a Hall thruster with an external cathode. I: numerical simulations. *Plasma Sources Sc. Technol.*, 2020, vol. 29, no. 3, art. 035011. DOI: https://doi.org/10.1088/1361-6595/ab6c7e

[20] Mikellides I.G., Ortega A.L., Chaplin V.H., et al. Facility pressure effects on a hall thruster with an external cathode. II: theoretical model of the thrust and the significance of Azimuthal asymmetries in the cathode plasma. *Plasma Sources Sc. Technol.*, 2020, vol. 29, no. 3, art. 035010. DOI: https://doi.org/10.1088/1361-6595/ab6c7f

[21] Azziz Y. Experimental and theoretical characterization of a hall thruster plume. PhD Dissertation, Cambridge, Massachusetts Inst. of Technology, 2007.

[22] Khartov S., Metois P., Nadiradze A., et al. Simulation tools for the plasma propulsion and satellite environment. *52nd Int. Astronautical Cong.*, *1-5 October 2001*, Toulouse, France, 2001, art. IAF-01-S.4.08

[23] Korsun A.G., Tverdokhlebova E.M. The characteristics of the EP exhaust plume in space. *AIAA/ASME/SAE/ASEE Joint Propulsion Conf.*, 1997.
DOI: https://doi.org/10.2514/6.1997-3065

[24] Korsun A.G., Tverdokhlebova E.M., Gabdullin F.F. The distinction between the EP plume expansion in space and in vacuum chamber. *29th Int. Electric Propulsion Conf.*, 2005, art. IEPC-2005-073.

[25] Nadiradze A.B., Kharov S.A. A 3D model calculating sputtering and depositing processes under electric propulsion thruster testing in a vacuum chamber. *Proc. 29th Int. Electric Propulsion Conf.*, 2005, art. IEPC-2005-77

[26] Pacros A. Instruments design and testing for a hall thruster plume experiment on the space shuttle. Cambridge, Massachusetts Institute of Technology, 2002.

[27] Barkalov E.E., Veselovzorov A.N., Pogorelov A.A., et al. Composition of the beam of an SPT-100 stationary plasma thruster. *Instrum. Exp. Tech.*, 2008, vol. 51, no. 2, pp. 263–267. DOI: https://doi.org/10.1134/S002044120802019X

[28] Toropov G.P., Khartov S.A. Model of plasma thruster jet propagation in vacuum chamber during testing considering electric field influence. *Vestnik MAI* [MAI Aerospace Journal], 2011, no. 2 (in Russ.).
Available at: http://vestnikmai.ru/publications.php?ID=26091&eng=N

[29] Nadiradze A.B., Frolova Yu.L., Zuev Yu.V. Conical plume model calibration of the stationary plasma thruster by the thruster integral parameters. *Vestnik MAI* [MAI Aerospace Journal], 2019, no. 4 (in Russ.).
Available at: http://vestnikmai.ru/publications.php?ID=110984

[30] Gorshkov O.A., Shagayda A.A. Studying impurities in the plasma jet of a closed-electron-drift thruster. *Tech. Phys. Lett.*, 2008, vol. 34, no. 4, pp. 354–357.
DOI: https://doi.org/10.1134/S106378500804024X

Nadiradze A.B. — Dr. Sc. (Eng.), Professor, Department of Electric Rocket Engines, Power and Energy-Physical Plants, Moscow Aviation Institute (National Research University) (Volokolamskoe shosse 4, Moscow, 125993 Russian Federation).

Frolova Yu.L. — Analytic, VNIIMS (Ozernaya ul. 46, Moscow, 119361 Russian Federation).

Please cite this article as:

Nadiradze A.B., Frolova Yu.L. Methods for assessing parameters of the stationary plasma engine plume multifractional model based on the results of probe measurements. *Herald of the Bauman Moscow State Technical University. Series Mechanical Engineering*, 2021, no. 1 (136), pp. 53–67.
DOI: https://doi.org/10.18698/0236-3941-2021-1-53-67